GaN Electronics For High Power, High Temperature Applications

by S. J. Pearton, F. Ren, A. P. Zhang, G. Dang, X. A. Cao, H. Cho, C. R. Abernathy, J. Han, A. G. Baca, C. Monier, P. Chang, R. J. Shul, L. Zhang, J. M. Van Hove, P. P. Chow, J. J. Klaassen, C. J. Polley, A. M. Wowchack, D. J. King, S. N. G. Chu, M. Hong, A. Y. Polyakov, N. B. Smirnov, A. V. Govorkov, J.-I. Chyi, C.-M. Lee, T.-E. Nee, C.-C. Chuo, G. C. Chi, and J. M. Redwing

The commercialization of blue, green, and white GaN-based light-emitting diodes and violet laser diodes has created tremendous interest both from an applications viewpoint and for the basic science of the AlGaInN materials system. The fact that extremely efficient light emission can be achieved in heteroepitaxial layers of these materials grown on lattice mismatched substrates such as sapphire is counter to the experience of almost 40 years of semiconductor light source technology.[1] The high dislocation density in these heteroepitaxial layers (10^{10}-10^{11} cm^{-2}) is clearly not as deleterious as in more conventional materials systems such as GaAs/AlGaAs, InP/InGaAsP, and GaAsP/GaP. While large diameter GaN bulk substrates are not commercially available and will not be in the foreseeable future, ingenious methods of creating quasi-substrates have been developed. These include lateral overgrowth of GaN on dielectric-patterned sapphire or SiC substrates, in which the growth of GaN up and over the dielectric pattern creates regions of much lower dislocation density; or growth of thick (100 µm) GaN epitaxial layers on mismatched substrates, followed by separation from the substrate to create a free-standing GaN substrate. Photonic devices fabricated on these lower-defect GaN regions have even better optical output and reliability than those fabricated on highly defective regions.

There are also numerous advantages of the AlGaInN system for high power electronics, including wide bandgaps for high voltage and temperature operation, good transport properties, the availability of heterostructures, and finally the experience base accumulated during the development of nitride-based light-emitting diodes and lasers. Most of the work on nitride-based electronics has focused on AlGaN/GaN high electron mobility transistors for power microwave applications,[2] but there are potential advantages to the use of bipolar transistors (either heterojunction bipolar transistors or bipolar junction transistors) in some applications because of their higher current densities, better linearity and more uniform threshold voltages. GaN/AlGaN bipolar transistors are an attractive option for various satellite, radar, and communications applications in the 1-5 GHz frequency range, at temperatures > 400°C and powers > 100 W. Traditional Si-based technologies cannot support such requirements, but the wide bandgap GaN system is capable of reaching this performance level.

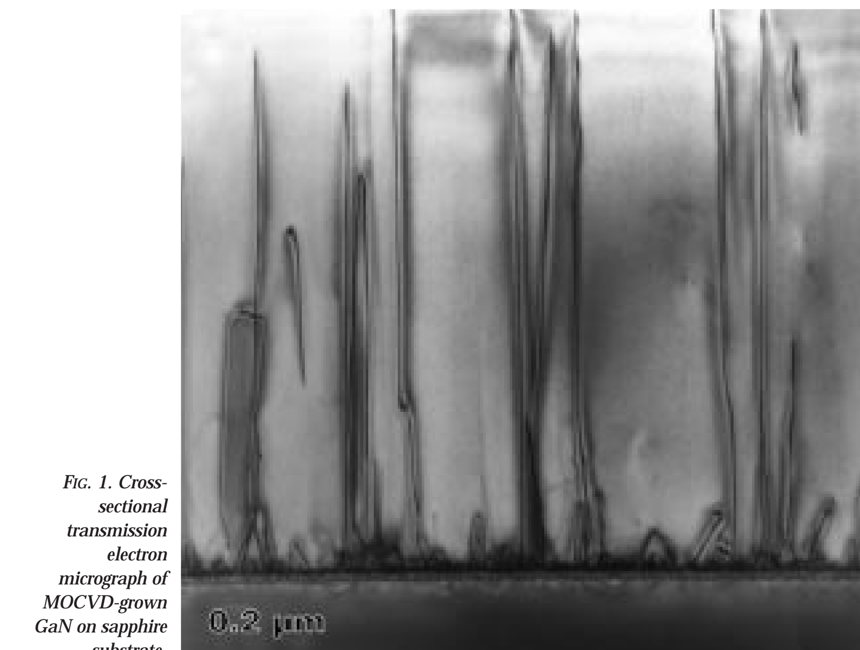

Fig. 1. Cross-sectional transmission electron micrograph of MOCVD-grown GaN on sapphire substrate.

In addition, there is a strong interest in developing high current, high voltage switches in the AlGaN materials system for applications in the transmission and distribution of electric power and in the electrical sub-systems of emerging vehicle, ship, and aircraft technology. It is expected that packaged switches made from AlGaN may operate at temperatures in excess of 250°C without liquid cooling, thereby reducing system complexity, weight, and cost. In terms of voltage requirements, there is a strong need for power quality enhancement in the 13.8 kV class, while it is estimated that availability of 20-25 kV switches in a single unit would cause a sharp drop in the cost of power flow control circuits. Schottky and p-i-n rectifiers are an attractive vehicle for demonstrating the high voltage performance of different materials systems and blocking voltages in the 3-5•9 kV range have been reported in SiC devices. The reverse leakage current in Schottky rectifiers is generally far higher than expected from thermionic emission, most likely due to defect states around the contact periphery. To reduce this leakage current and prevent breakdown by surface flash-over, edge termination techniques such as guard rings, field plates, beveling, or surface ion implantation are necessary. However, in the few GaN rectifiers reported so far, there has been little effort on employing edge termination methods, and no investigation of

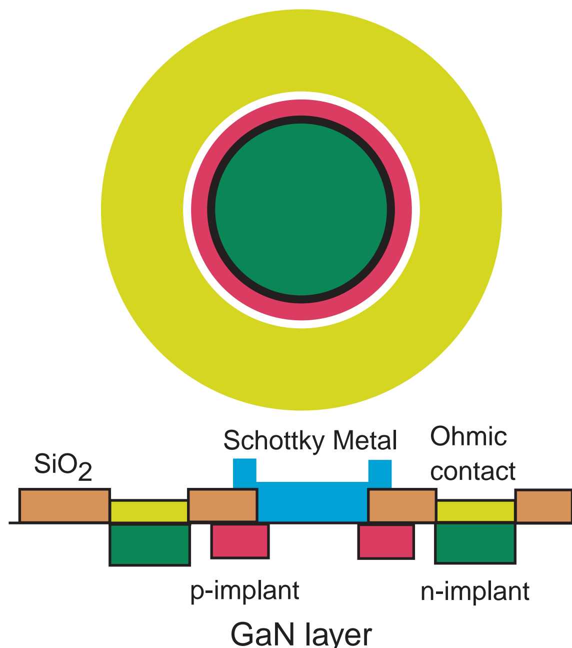

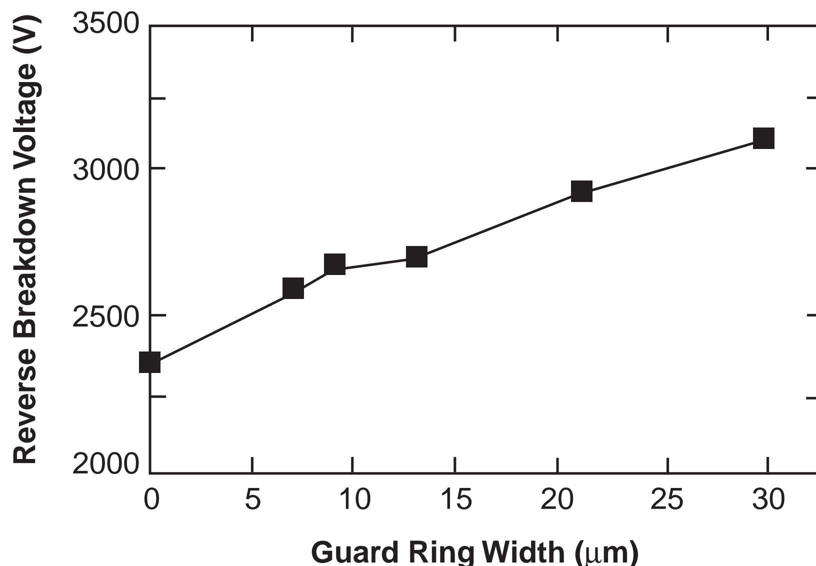

Fig. 2. (top) View of rectifiers with p-type guard rings; (bottom) Variation of V_{RB} with guard ring width.

the effect of increasing the bandgap by use of AlGaN.

Here we detail recent results in GaN power electronic devices, including Schottky rectifiers, heterojunction bipolar transistors (HBTs), bipolar junction transistors (BJTs), metal oxide semiconductor field effect transistors (MOSFETs), and high electron mobility transistors (HEMTs). The pace of advancement of these technologies has been remarkably rapid in the past two years.

GaN Rectifiers

For these devices, GaN was grown on c-plane Al_2O_3 substrates by metal organic chemical vapor deposition (MOCVD) using trimethylgallium and ammonia as the precursors. For vertically-depleting devices, the structure consisted of a 1μm n^+ ($3x10^{18}$ cm^{-3}, Si-doped) contact layer, followed by undoped (n = $2.5x10^{16}$ cm^{-3}) blocking layers which ranged from 3 to 11 μm thick. A cross-sectional transmission electron micrograph is shown in Fig. 1. Note the high dislocation density in this heteroepitaxial material. These samples were formed into mesa diodes using inductively coupled plasma (ICP) etching with Cl_2/Ar discharges (300 W source power, 40 W rf chuck power). The dc self-bias during etching was –85 V. To remove residual dry etch damage, the samples were annealed under N_2 at 800°C for 30 s. Ohmic contacts were formed by lift-off of electron-beam evaporated Ti/Al, annealed at 700°C for 30 s under N_2 to minimize the contact resistance. Finally, the rectifying contacts were formed by lift-off of electron-beam evaporated Pt/Au. Contact diameters of 60-1100 μm were examined.

For laterally-depleting devices, the structure consisted of ~3 μm of resistive (10^7 ohms per square) GaN. To form ohmic contacts, Si^+ was implanted at $5x10^{14}$ cm^{-2}, 50 keV into the contact region and activated by annealing at 150°C for 10 s under N_2. The resulting n-type carrier concentration was $1x10^{19}$ cm^{-3}. The ohmic and rectifying contact metallization was the same as described above.

Three different edge termination techniques were investigated for the planar diodes: (1) use of a p-guard ring formed by Mg^+ implantation at the edge of the Schottky barrier metal. In these diodes the rectifying contact diameter was held constant at 124 μm, while the distance of the edge of this contact from the edge of the ohmic contact was 30 μm in all cases; (2) use of p-floating field rings of width 5 μm to extend the depletion boundary along the surface of the SiO_2 dielectric, which reduces the electric field crowding at the edge of this boundary. In these structures a 10 μm wide p-guard ring was used, and 1-3 floating field rings employed; and (3) use of junction barrier controlled Schottky (JBS) rectifiers, *i.e.,* a Schottky rectifier structure with a p-n junction grid integrated into its drift region.

In all of the edge-terminated devices, the Schottky barrier metal was extended over an oxide layer at the edge to further minimize the field crowding, and the guard and field rings formed by Mg^+ implantation and 1100°C annealing.

Figure 2 (top) shows a schematic of the planar diodes fabricated with the p-guard rings, while the bottom of the figure shows the influence of guard ring width on the reverse breakdown voltage V_{RB} at 25°C. Without any edge termination, V_{RB} is ~2300 V for these diodes. The forward turn-on voltage was in the range 15-50 V, with a best on-resistance R_{ON} of 0.8 Ωm^2. The figure of merit $(V_{RB})^2/R_{ON}$ was 6.8 MW cm^{-2}. As the guard-ring width was increased, we observed a monotonic increase in V_{RB}, reaching a value of ~3100 V for 30 μm wide rings. The figure of merit was 15.5 MW cm^{-2} under these conditions. The reverse leakage current of the diodes was still in the nA range at voltages up to 90% of the breakdown value. Similar results were obtained with the field rings or JBS control.

The results shown in Fig. 2 are convincing evidence that proper design and implementation of edge termination methods can significantly increase V_{RB} in GaN diode rectifiers and will play an important role in applications at the very highest power levels. For example, the target goals for devices intended to be used for transmission and distribution of electric power or in single-pulse switching in the subsystem of hybrid-electric contact vehicles are 25 kV standoff voltage, 2 kA conducting current and forward voltage drop < 2% of the standoff voltage. At these power levels, it is expected that edge termination techniques will be essential for reproducible operation.

To place our results in the context of reported SiC Schottky diode performance in the literature, Fig. 3 shows a plot of specific on-resistance versus reverse breakdown voltage for SiC and GaN diodes, together with the calculated (theoretical) performance. The 3.1 kV result for GaN reported here is still well below the theoretical value, indicating that further improvements in processing and materials are needed. Some reported SiC devices perform close to the theoretical limit, reflecting the greater maturity of this technology at present.

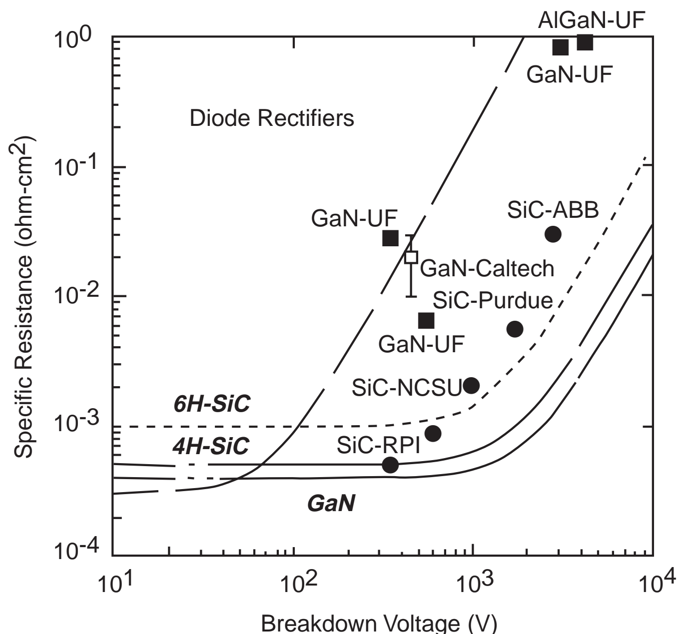

Fig. 3. On-resistance versus blocking voltage for SiC and GaN diode rectifiers. The performance limits of Si, SiC and GaN devices are shown by the dashed line for the 6H polytype of SiC, or by the solid line for the 4H polytype of SiC and for GaN.

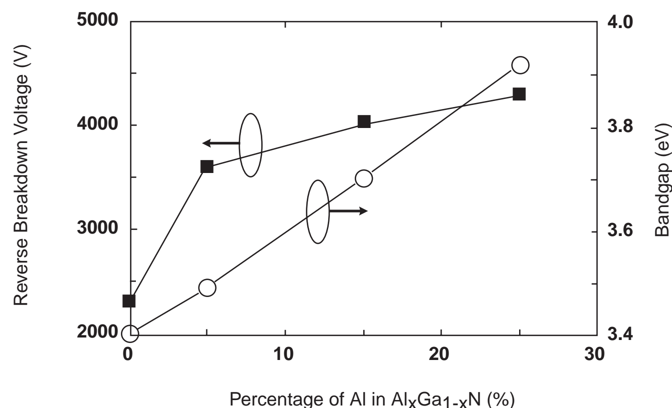

Fig. 4. Variation of V_{RB} in $Al_xGa_{1-x}N$ rectifiers without edge termination, as a junction of Al concentration. The bandgaps for the AlGaN alloys are also shown.

AlGaN Rectifiers

The undoped $Al_xGa_{1-x}N$ layers were grown by atmospheric pressure MOCVD at 1040°C (pure GaN) or 1100°C (AlGaN) on (0001) oriented sapphire substrates. The precursors were trimethylgallium, trimethlygaluminum and ammonia, with H_2 used as a carrier gas. The growth was performed on either GaN (in the case of GaN active layers) or AlN (in the case of AlGaN active layers) low temperature buffers with nominal thickness of 200 Å. The active layer thickness was ~2.5 μm in all cases and the resistivity of these films was of order 10^7 Ωcm. To form ohmic contacts in some cases, Si^+ was implanted at $5x10^{14}$ cm^{-2}, 50 keV into the contact region and activated by annealing at 1150°C for 10 s under N_2. The contacts were then formed by lift-off of e-beam evaporated Ti/Al/Pt/Au annealed at 700°C for 30 s under N_2. The rectifying contacts were formed by lift-off of e-beam evaporated Pt/Ti/Au (diameter 60-1100 μm). The on-resistance of the AlGaN diodes was higher than for pure GaN, due to higher ohmic contact resistance. The lowest R_{ON} achieved was 3.2 Ωcm^2, leading to a figure of merit of ~5.5 MW cm^{-2}.

Figure 4 shows the variation of V_{RB} with Al percentage in the AlGaN active layers of the rectifiers. In this case we are using the V_{RB} values from diodes without any edge termination or surface passivation. The calculated bandgaps as a function of Al composition are also shown, and were obtained from the relation

$$E_g(x) = E_gGaN(1-x) + E_gAlN \cdot x - bx(1-x)$$

where *x* is the AlN mole fraction and *b* is the bowing parameter with a value of 0.96 eV. Note that V_{RB} does not increase in a linear fashion with bandgap. In a simple theory, V_{RB} should increase as $(E_g)^{1.5}$, but it has been empirically established that factors such as impact ionization coefficients and other transport parameters need to be considered and that consideration of E_g alone is not sufficient to explain measured V_{RB} behavior. The fact the V_{RB} increases less rapidly with E_g at higher AlN mole fractions may indicate increasing concentrations of defects that influence the critical field for breakdown.

The reverse I-V characteristics of all of the rectifiers showed $I \propto V^{0.5}$ over a broad range of voltage (50-2000 V), indicating that Shockley-Read-Hall recombination is the dominant transport mechanism. The current density in all devices was in the range 5-10x10^{-6} A$\cdot$cm^{-2} at 2 kV. At low biases (≤ 25 V) the reverse current was proportional to the perimeter of the rectifying contact, suggesting that surface contributions are the most important in this voltage range. For higher biases, the current was proportional to the area of the rectifying contact. Under these conditions, the main contribution to the reverse current is from under this contact, *i.e.,* from the bulk of the material. It is likely that the high defect density in heteroepitaxial GaN is a primary

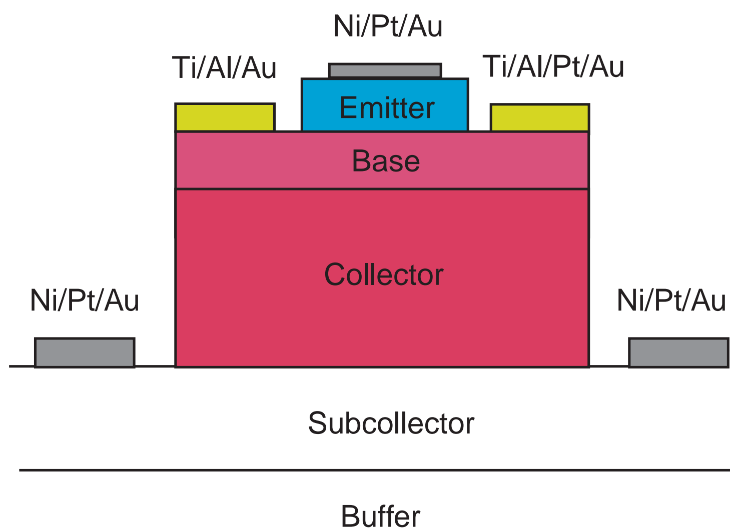

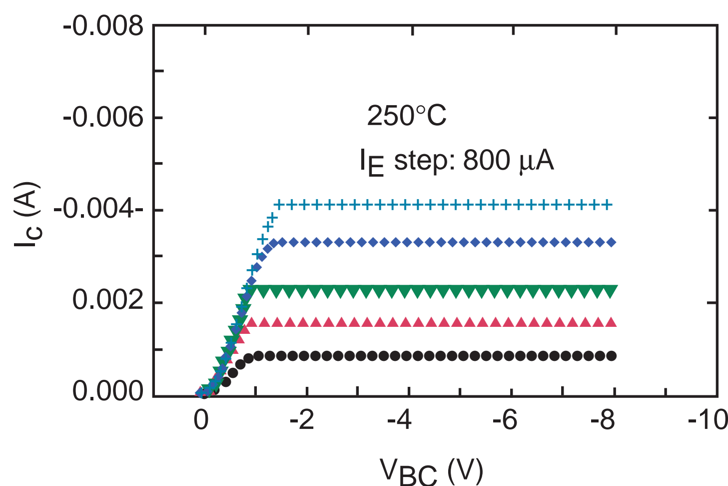

FIG. 5. Schematic of p-n-p GaN BJT (top) and common-base characteristics at 250°C (bottom).

cause of this current. The forward I-V characteristics showed that the current density was proportional to exp (-eV/2kT) at the lowest voltages (up to current densities of ~5×10^{-4} A·cm^{-2}) and to exp (-eV/1.5kT) at the higher voltages (current densities in the range 10^{-3} to 1.5×10^{2}A·cm^{-2}). These results are consistent with Shockley-Read-Hall recombination as the dominant mechanism at low bias, followed by diffusion current at higher voltage. Qualitatively similar behavior has been reported previously for SiC rectifiers.

When pushed beyond breakdown, the diodes invariably failed at the edges of the rectifying contact. As described earlier, the use of metal field plate contact geometries with SiO_2 as the insulator and either guard rings or floating field rings significantly increased V_{RB}. These rectifiers generally did not suffer irreversible damage to the contact upon reaching breakdown and could be remeasured many times.

GaN/AlGaN Heterojunction Bipolar Transistors

Both n-p-n and p-n-p HBTs have been fabricated with emitter contact diameters in the range 50-100 μm. HBT power microwave amplifiers are mostly designed on common-emitter or common-base operation. The current gain is greater than unity only in the common-emitter mode, but the common-base mode is attractive because of the possibility of appreciable power gain through the impedance transformation offered by this amplifier.

In all of our devices we have observed that the saturated collector current was nearly equal to the emitter current, which indicates a high emitter injection efficiency. Gummel plots showed dc current gains of 15-20 at room temperature. In many of the devices it is difficult to obtain common-emitter operation due to leakage in the collector-base junction, and at all temperatures (25-300°C) the junction ideality factors for both emitter-base and collector-base junctions were close to 2, indicative of significant recombination. By removing the base contact we observed no collector current, which confirms the transistor modulation.

For n-p-n devices the performance is limited by the high base resistance, which originates from the deep ionization level of the Mg acceptors. In these devices we have achieved maximum current densities of 2.55 kA·cm^{-2} at V_{BC} = 8 V, corresponding to power densities of 20.4 kW·cm^{-2}.

There are two advantages to the p-n-p configuration for AlGaN/GaN HBTs. First, there is a larger emitter-base energy bandgap offset than in n-p-n structures, and second, the base resistance will be much lower due to higher doping level achievable in n-type material. The best p-n-p HBTs can be operated up to current densities of over 2 kA·cm^{-2} at 25 V, corresponding to power densities above 50 kW·cm^{-2}.

GaN Bipolar Junction Transistors

The epitaxial growth of BJTs is simpler than for HBTs because the emitter layer is comprised of GaN rather than AlGaN. In our n-p-n devices we have achieved maxium current densities of 3.6 kA·cm^{-2} at a collector-base voltage of 15 V, corresponding to a power density of 54 kW·cm^{-2}. The maximum commom-emitter dc current gain was ~15 for temperatures up to 300°C. The operation of both GaN BJTs and GaN/AlGaN HBTs was simulated using a program based on the drift-diffusion model. This simulation showed that at low current densities the HBT enjoys an advantage due to the conduction band offset, but that at higher current densities the results converged. This suggests that simple BJTs are useful as power devices.

Figure 5 (top) shows a schematic of a completed p-n-p GaN BJT, in which the mesas were formed by Cl_2/Ar ICP etching under low damage conditions. Common-base current-voltage characteristics at 250°C are shown at the bottom of the figure. The dc characteristics were measured up to a collector-base voltage (V_{BC}) of 65V in the common-base mode. A stable current density of 204 A·cm^{-2} was run at this voltage, corresponding to a power density of 40 kW·cm^{-2}. These values can clearly be increased by optimized design of layer structure and mask layout. The devices showed little fall-

Table I. Historical development of GaN-based electronics.

Year	Event	Authors
1969	GaN by hydride vapor phase epitaxy	Maruska and Tietjen
1971	MIS LEDs GaN by MOCVD	Pankove *et al.* Manasevit *et al.*
1974	GaN by MBE	Akasaki and Hayashi
1983	AlN intermediate layer by MBE	Yoshida *et al.*
1986	Specular films using AlN buffer	Amano *et al.*
1989	p-type Mg-doped GaN by LEEBI and GaN p-n junction LED	Amano *et al.*
1991	GaN buffer layer by MOCVD	Nakamura
1992	Mg activation by thermal annealing AlGaN/GaN two-dimensional electron gas	Nakamura *et al.* Khan *et al.*
1993	GaN MESFET AlGaN/GaN HEMT Theoretical prediction of piezoelectric effect in AlGaN/GaN	Khan *et al.* Khan *et al.* Bykhovski *et al.*
1994	InGaN/AlGaN DH blue LEDs (1 cd) Microwave GaN MESFET Microwave IIFET, MISFET GaN/SiC HBT	Nakamura *et al.* Binari *et al.* Binari *et al.*; Khan *et al.* Pankove *et al.*
1995	AlGaN/GaN HEMT by MBE	Ozgur *et al.*
1996	Doped channel AlGaN/GaN HEMT Ion-implanted GaN JFET 340 V VGD AlGaN/GaN HEMT 1st blue laser diode	Khan *et al.* Zolper *et al.* Wu *et al.* Nakamura and Fosal
1997	Quantification of piezoelectric effect AlGaN/GaN HEMT on SiC 1.4 W @ 4 GHz 0.85 W @ 10 GHz 3.1 W/mm at 18 GHz	Asbeck *et al.* Binari *et al.*; Ping *et al.* Gaska *et al.* Thibeault *et al.* Siram *et al.* Wu *et al.*
1998	3.3 W p-n junction in LEO GaN HEMT in LEO GaN 6.8 W/mm (4 W) @ 10 GHz HEMT on SiC 10^{-4} Hooge factor for HEMT on SiC 1st AlGaN/GaN HBT 1st GaN MOSFET	Sullivan *et al.* Kozodoy *et al.* Mishra *et al.* Sheppard *et al.* Levinshtein *et al.* McCarthy *et al.* Ren *et al.* Ren *et al.*
1999	9.1 W/mm @ 10 GHz HEMT on SiC GaN BJT (n-p-n)	Mishra *et al.* Yoshida *et al.*
2000	4.3 kV AlGaN rectifier p-n-p GaN/AlGaN HBT p-n-p GaN BJT	Zhang *et al.* Zhang *et al.* Zhang *et al.*

off in performance at temperatures up to 250°C.

GaN Metal Oxide Semiconductor Field Effect Transistors

A GaN depletion-mode metal oxide semiconductor field effect transistor was demonstrated, using Ga_2O_3 (Gd_2O_3) as the gate dielectric, similar to the approach reported for GaAs and InGaAs. The MOS gate reverse breakdown voltage was > 35 V, significantly higher than obtained using a simple Pt Schottky gate on the same material. A maximum extrinsic transconductance of 15 $mS \cdot mm^{-1}$ was obtained at a drain-source voltage, V_{DS} = 30 V and device performance was limited by the contact resistance. A unity current gain cut-off frequency, f_T, and maximum frequency of oscillation, f_{MAX}, of 3.1 and 10.3 GHz, respectively, were measured at V_{DS} = 25 V and gate-source voltage, V_{GS} = -20 V. The device performance can be improved by optimizing the layer structure using a thin and heavily doped channel layer, which will reduce the contact resistance and enhance the transconductance.

AlGaN/GaN High Electron Mobility Transistors

DC Performance—AlGaN/GaN transistor development has followed the material improvements driven by photonic devices such as LEDs and laser diodes. Table I outlines the historical evolution for this technology and the key developments.

The first reports of GaN based transistors were by Khan *et al.* with the demonstration of a GaN metal semiconductor field effect transistor (MESFET) and an AlGaN/GaN HEMT.[2] Both transistors had gate lengths of 4 μm with the MESFET having a transconductance (g_m)of 23 mS/mm and a maximum drain-source current (I_{DS}(max))of ~180 mA/mm (@V_{GS} = 0 V, V_{DS} = 20 V). The AlGaN/GaN HEMT achieved a g_m of 28 mS/mm at 300 K (46 mS/mm at 77 K) and I_{DS}(max) of ~50 mA/mm (@V_{GS} = 0.5 V, V_{DS} = 25 V). The HEMT structure had a two dimensional electron gas (2DEG) mobility of 563 cm^2/V s at 300 K and 1517 cm^2/Vs at 77 K. The first microwave results were published by Binari *et al.*, for a GaN MESFET with a demonstrated f_t of 8 GHz and a f_{max} of 17 GHz for a gate length of 0.7 μm.[3]

Since the early results, significant improvements have been made in materials quality and device pro-

cessing. AlGaN/GaN 2DEG mobilities up to 2019 cm^2/Vs have been reported for growth on 6H-SiC substrates and ~1600 cm^2/Vs for growth on sapphire substrates. The saturation current has been pushed to 1.6 A/mm and the transconductance has reached 340 mS/mm.[2]

Microwave Small and Large Signal Performance—Improvements in the small signal microwave performance of AlGaN/GaN HEMTs have tracked the dc improvements. The present state-of-the-art for unity current cut-off frequency (f_t) is 75 GHz by Eastman and co-workers at Cornell University.[4] Large signal power results for HEMT on SiC substrates include total power of 9.1 W (2-mm-wide gate) at 10 GHz with 10 dB of gain with a power density of 6.8 W/mm (4.1 W/mm at 16 GHz) measured on smaller devices.[5] At 18 GHz, a power density of 3.1 W/mm has been achieved on a sapphire substrate. Total power results have also been pushed up to 7.6 W, achieved at 4 GHz for HEMTs grown on sapphire and flip-chip mounted on AlN carriers.[6] These large signal results, however, are still not up to the level one would predict from the dc characteristics and the small signal performance of up to ~10 W/mm at 10 GHz. In some cases, the performance shortfall is evident in current and gain compression at high applied voltages. This compression is due to traps in the band gap, possibly at the surface, in the AlGaN barrier, or in the GaN buffer. Presently, the origin of the traps is still being studied, however, a similar phenomenon was observed in the early GaAs device work and later overcome. In the GaAs case, the effect was due to surface states but this may not be the case with the AlGaN/GaN system.

Elevated Temperature Performance—The group III nitride semiconductors have been considered as ideal candidates for high temperature electronic devices due to their large band gap and resulting low thermal carrier generation rate. For this potential to be realized, defect levels in the band gap must be reduced because they will enhance undesirable dark and shunt currents. This can be seen in the temperature dependence of conduction reported by Khan *et al.*,[2] where a AlGaN/GaN HEMT demonstrated a large shunt current apparently resulting from defect assisted conduction in the GaN buffer layer already at 200°C. Subsequently a GaN MESFET with an improved semi-insulating buffer was shown, by Binari *et al.*, to maintain reasonable pinch-off characteristics at 400°C.[3] When taken to 500°C, the MESFET gate electrode began to interact with the GaN surface and irreversibly degrade the transistor operation. An AlGaN/GaN HEMT has been further pushed to operate at 750°C by achieving a 1.0 eV activation energy for conduction in the buffer layer and employing a thermally stable Pt-Au gate contact.[7] More work is needed to optimize such elevated temperature operation, and device packaging must also be considered. ■

Summary

Tremendous progress has been made in advancing the growth, processing, and design of GaN power electronics in recent times. However, there are as yet no commercially-available devices and this may take another three to five years to occur.

Acknowledgments

The work at the various institutions has been supported by ONR (J. C. Zolper), DARPA (D. Radack), EPRI (J. Melcher), NSF (L. Hess), the U.S. Civilian R&D Foundation, the Russian Foundation for Fundamental Research, by BMDO, and the National Science Council of ROC. Sandia is a multiprogram laboratory operated by Sandia Corporation, a Lockheed-Martin company, for the U.S. Department of Energy.

References

1. S. Nakamura and G. Fasol, *The Blue Laser Diode*, Springer, Heidelberg (1997).
2. M. S. Shur and M. A. Khan, in *GaN and Related Materials II*, S. J. Pearton, Editor, Gordon and Breach, New York (2000).
3. S. C. Binari, L. B. Rowland, W. Kruppa, G. Kelner, K. Doverspike, and D. K. Gaskill, *Electron. Lett.*, **30**, 1248 (1994).
4. L. F. Eastman, K. G. Chu, J. Smart, and J. R. Shealy, *Mater. Res. Soc. Symp. Proc.*, **512**, 3 (1998).
5. S. T. Sheppard, K. Doverspike, W. L. Pribble, S. T. Allen, and J. W. Palmour, 56th Device Research Conference, Charlottesville, VA, June 1998.
6. Y.-F. Wu, B. J. Thibeault, B. P. Keller, S. Keller, S. P. DenBaars, and U. K. Mishra, Topical Workshop on Heterostructure Electronics, Kanagawa, Japan, Sept 1998.
7. L. Daumiller, L. Kirchner, M. Kamp, K. J. Eheling, L. Pond, C. E. Weitzel, and E. Kohn, 56th Device Research Conference, Charlottesville, CA, June 1998.

About the Authors

S. J. Pearton, F. Ren, A. P. Zhang, G. Dang, X. A. Cao, H. Cho, and C. R. Abernathy are with the University of Florida in Gainesville, Florida.

J. Han, A. G. Baca, C. Monier, P. Chang, R J. Shul, and L. Zhang are with Sandia National Laboratories, Albuquerque, New Mexico.

J. M. Van Hove, P. P. Chow, J. J. Klaassen, C. J. Polley, A. M. Wowchack, and D. J. King are with SVT Associates in Eden Prairie, Minnesota.

S. N. G. Chu and M. Hong are with Bell Laboratories, Lucent Technologies, in Murray Hill, New Jersey.

A. Y. Polyakov, N. B. Smirnov, and A. V. Govorkov are with the Institute of Rare Metals in Moscow, Russia.

J.-I. Chyi, C.-M. Lee, T.-E. Nee, C.-C. Chuo, and G. C. Chi are with National Central University in Chung-Li, Taiwan.

J. M. Redwing is with Pennsylvania State University in College Park, Pennsylvania.